農業工程學報　第 47 卷第 2 期
中華民國 90 年 6 月出版

Journal of Chinese Agricultural Engineering
Vol. 47, No. 2, June 2001

等溫狀態強制通風空間壁噴流之空氣流特徵

Airflow Characteristics of Plane Wall Jet Diffused into a Forced Ventilated Enclosure under Isothermal Condition

國立宜蘭技術學院土木工程系副教授

喻　　新

Hsin Yu

摘　　要

通風系統常利用條狀天花板入口方式控制室內環境，爲瞭解此種壁噴流之流場特徵，本研究應用模型試驗以驗證其噴流表現。由試驗之結果得知最大流速之衰減、最大流速位置、流速分佈剖面以及流場擴張均與前人之分析結果相符。室內侷限氣流型態亦可由氣流射程之計算以及氣流相對牆面之影響而估計。上述實驗與理論分析結果相符之氣流特徵將有助於推測等溫壁噴流在侷限空間之表現方式。未來在動物佔據區之噴流特徵，以及非等溫狀態之侷限壁噴流特徵均是值得研究的重點。

關鍵詞：通風，空氣流，壁噴流，等溫狀態。

ABSTRACT

Ventilation controlling indoor environment depends on air-jet diffused from a ceiling slot into a confined enclosure. The characteristics of plane wall jet were investigated by scale-model study to recognize the performance of air-jet. The maximum airspeed decay, the maximum airspeed position, the velocity profiles, and the spread of air-jet agreed with the literature analytical results. The airflow pattern of confined air-jet was predicted by using the jet throw calculation and the effect of opposite wall. These agreements of air-jet characteristics are helpful to predict the performance of isothermal plane wall jet diffused into a confined enclosure. The air-jet characteristics of animal occupied zone in confined enclosure and of the air-jet under non-isothermal condition are important subjects for future study.

Keywords: Ventilation, Airflow, Plane wall jet, Isothermal condition.

1. INTRODUCTION

The characteristics of ventilated airflow inside an enclosure affects air distribution, the thermal environment, and contaminant concentration (Awbi, 1991). The air-jet diffused from a ceiling slot into a confined enclosure behaves like a plane wall jet initially that is bounded by a surface on one side and is parallel to the surface. The air-jet then is issued into a room confined by solid boundaries and is influenced by reverse flow created by the air-jet itself. The theoretical and experimental investigations of confined plane wall jets is much more difficult than the plane free jet (Szucs, 1980).

The plane wall jet is two-dimensional with only a potential core, characteristic decay region, and terminal region as show in Figure 1 (Awbi, 1991). As the air-jet exits from the inlet, a shear layer develops on the fluid side due to the "no-slip" condition at the solid boundary (Rajaratnam, 1976). A boundary layer develops on the wall side and the shear layer expands on the free boundary. The potential core region is consumed when the boundary and shear layers meet. The length of potential core extends 5 to 10 equivalent opening diameter depends on the type of opening. The centerline velocity is constant and equal to the supply velocity in this region as:

$$U_{\max} = U_d \quad \text{.....(1)}$$

Beyond this region, a fully developed flow in the characteristic decay region is established (Rajaratnam, 1976). The centerline velocity decay begins to gradually decrease so that:

$$\frac{U_{\max}}{U_d} \propto \frac{1}{x^n} \quad \text{.....(2)}$$

where x= the distance from the supply, n= an index which has a value between 0.33 and 1.0 depend on the shape of supply opening.

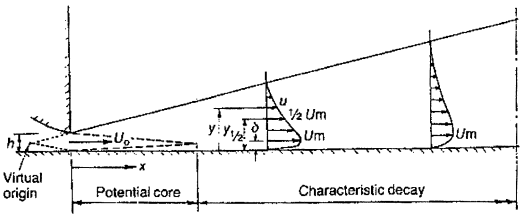

Figure 1. Schematic of a plane wall jet (Awbi, 1991).

Terminal region is a region of rapid dispersion. The centerline velocity decays with reciprocal of the squared distance as:

$$\frac{U_{\max}}{U_d} \propto \frac{1}{x^2} \quad \text{.....(3)}$$

Rajaratnam (1976) described the centerline velocity decay for a plane wall jet in the characteristic decay region by averaging the curves from different experimental data sources resulting in the following:

$$\frac{U_{\max}}{U_d} = 3.50\sqrt{\frac{h}{x}} \quad \text{.....(4)}$$

Albright(1990) stated the centerline velocity decay of plane wall jet as :

$$\frac{U_{\max}}{U_d} = 2.76\sqrt{\frac{h}{x}} \quad \text{.....(5)}$$

ASHRAE(1993) suggested another expression of the centerline velocity decay of an air-jet with ceiling linear outlet type as:

$$\frac{U_{\max}}{U_d} = \sqrt{\frac{K' h}{x}} \quad \text{.....(6)}$$

where K'=5.5. The above expression has a similar form as equation (4).

Rajaratnam (1976) expressed the non-dimensional velocity profile of a turbulent plane wall jet by the empirical expression

$$\frac{U}{U_{\max}} = 1.48\eta^{1/7}[1 - erf(0.68\eta)] \quad \text{.....(7)}$$

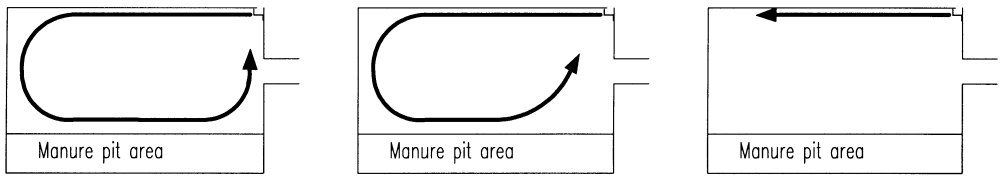

Figure 2. Categories of airflow pattern for isothermal condition (Jin and Ogilvie, 1990).

where $\eta = y / y_{1/2}$ and $y_{1/2} = 0.068(x - 10h)$.

Schwarz and Cosart (1961) described this profile as:

$$\frac{U}{U_{\max}} = \exp[-0.937(\eta - 0.14)^2] \quad \text{.....(8)}$$

Awbi (1991) concluded that Rajaratnam's equation gave better agreement with experimental data for $\eta \geq 0.14$.

The spread gradient of the position of half the maximum airspeed of plane wall jet at ceiling is:

$$\frac{dy_{1/2}}{dx} = C_{1/2} \quad \text{.....(9)}$$

where $C_{1/2}$ is ranged from 0.065 to 0.105 based on the previous researches (Sigalla, 1958; Schwarz and Cosart, 1961; Myers et al., 1963; Rajaratnam, 1976; Walker, 1977; Launder and Rodi, 1981; Albright, 1990).

Liu et al. (1994) derived a theoretical formula of $y_{1/2}$ as:

$$y_{1/2} = 0.073(x + x_0) \quad \text{.....(10)}$$

where x_0=12 from Schwarz and Cosart's(1961) statement.

Albright (1990) derived a formula of $y_{1/2}$ from equation (8) as:

$$y_{1/2} = \frac{\delta}{0.14} \quad \text{.....(11)}$$

The angle of spread of the plane wall jet is about 10º to 12º which is half value of a free wall jet (Albright, 1990; Etheridge and Sandberg, 1996).

The air-jet throw is the distance from the diffuser where the maximum velocity in the air-jet reaches a terminal velocity of 0.25 m/s for all diffusers except for ceiling slot diffusers, where the terminal velocity was proposed as 0.5 m/s (ASHRAE, 1993). The throw of plane wall jet could be derived from equation (4) as:

$$L_t = (\frac{U_d}{0.5})^2 C_w{}^2 h \quad \text{.....(12)}$$

Jin and Ogilvie (1990) identified three airflow zones that represented three types of airflow patterns in an empty 1:2 scale-model. The three zones were defined as the stagnant airflow zone (the mean floor airspeed remained below 0.1 m/s); the rotary airflow zone (air movement was fully rotary along the room perimeter), and the intermediate zone (the mean floor airspeed was greater than 0.1 m/s) (Figure 2).

Awbi and Setrak (1986) derived a theoretical expression of airflow pattern in an enclosure affected by the opposite wall as (Figure 3):

$$\frac{x_f}{h} = 0.52(\frac{L}{h})^{1.09} \quad \text{.....(13)}$$

Where x_f is the distance from supply of plane wall jets that the effect of the opposite wall is not detectable.

The objective of this study was to investigate characteristics of plane wall jet that diffused into a forced ventilated enclosure under isothermal

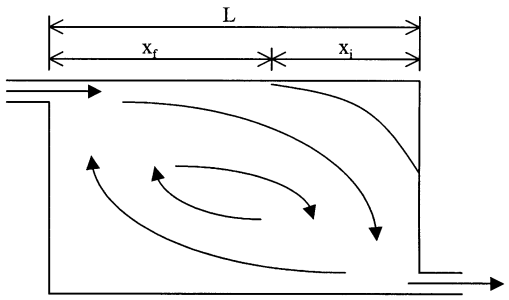

Figure 3. Effect of opposite wall (Awbi, 1991).

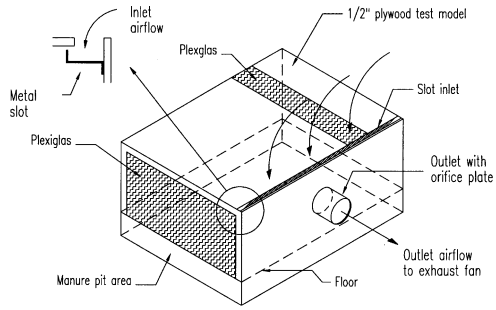

Figure 4. Scheme of experimental scale-model.

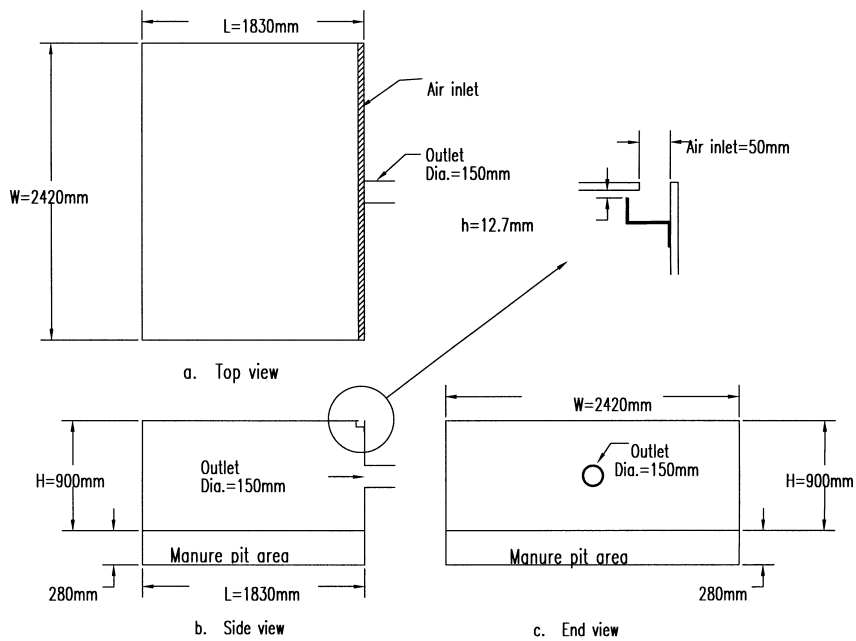

Figure 5. Dimensions of scale-models in different views.

condition through scale-model experiments. The results of model study compared with the theory and results from previous researchers to identify the reality of air-jet performance.

2. MATERIALS AND METHOD

The airflow patterns, air-jet penetration distance, and variation in velocity fields were measured by using airspeed measurements. The test chamber used is shown in Figure 4. The slot inlet width was the same as the width of the enclosure (W). The inlet aspect ratio was much larger than 20, and as a result, the airflow was treated as a two-dimensional wall jet without the effect of sidewalls (Forthmann, 1934).

The dimensions of model are shown in Figure 5. The scale model was made from 12.7mm thick (1/2 inch) plywood. The inner surfaces of the model were sanded and painted black. The front wall was made of Plexiglas to accommodate airflow visualization. Access holes were placed on the top ceiling along a cross line between inlet

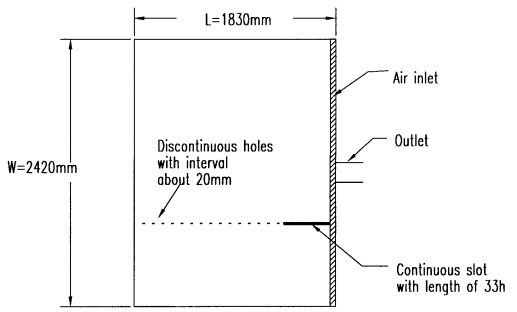

Figure 6. The plane-view of access holes on the top ceiling of test models.

wall and end wall at intervals of 20 mm, except for the area between the inlet and a distance of 33 h from the inlet where a continuous access slot was constructed to discretize air-jet development near the inlet (Figure 6).

Ductwork was constructed and fitted between the circular exhaust hole and an exhaust fan. Calibrated orifice plates were used to select desired airflow rates through model. A micromanometer (Model 1430; Dwyer Instruments, Inc.) was used to measure the pressure difference across the orifice to determine airflow rate. The orifice plates used in the pressure measurements were calibrated by a standard Venturi flow meter. The calibration curve showed good correlation by r^2>0.99.

Airspeed was measured using an omni-directional hot-film anemometer (Model 8470; TSI, Inc.) which was calibrated by the manufacture. The percentage of error was below 3%. A portable data acquisition system (Model CR10; Campbell Scientific, Inc.) was used to collect data. The acquiring period for each measurement was 180s and the sampling frequency was set at 16Hz. The average value over time, at a point, was used for analysis and presentation.

Many factors such as the accuracy of the measurement instruments, the limited sampling period, the accuracy of the room dimension, the accuracy in positioning the probe at the desired location, and the ambient environment affected the uncertainties of the experimental results.

The uncertainties of velocity measurements with hot-film anemometer were mainly due to natural convection over the probe. The uncertainties involved in the calibration and the A/D conversion were considered to be negligible. The uncertainties of ventilation due to the limited sampling period were negligible because of the sampling period in present study was much longer than the period needed to get steady average of velocity and turbulent kinetic energy. The uncertainty due to instrument were be $e_{u1} \approx \pm 15\%$, $\pm 5\%$, $\pm 3\%$, $\pm 1\%$ and $\pm 0.5\%$ for velocity of 0.05 to 0.1m/s, 0.1 to 0.15m/s, 0.15 to 0.25m/s, 0.25 to 0.5m/s and >0.5m/s, respectively (Zhang, 1991).

The dimensions of diffuser and room were accurate with $\pm$2mm and $\pm$1cm. The dimension error of room is about 1% of the room height and the dimension error of diffuser is negligible, i.e., $e_{u2} \approx \pm 1\%$ and $e_{u3} \approx 0$.

The probe position in the x and z directions were accurate with $\pm$5mm and $\pm$2.5mm. Since the errors were small compared to the room dimensions, the uncertainties were considered negligible in present study as $e_{u4} \approx 0$.

The fluctuation of the ambient air conditions was negligible for experiments were proceeded in a confined room of laboratory. The total uncertainties of measured quantities within experiments were $e_u \approx ({e_{u1}}^2 + {e_{u2}}^2 + e_{u3}^3 + e_{u4}^2)^{1/2} \approx \pm 15\%$, $\pm 5\%$, $\pm 3\%$, $\pm 1\%$ and $\pm 0.5\%$ for velocity of 0.05 to 0.1m/s, 0.1 to 0.15m/s, 0.15 to 0.25m/s, 0.25 to 0.5m/s and >0.5m/s, respectively.

3. RESULTS AND DISCUSSION

Jet airspeed decay

The maximum airspeed of plane wall jet with different airflow rate along the ceiling is shown in Figure 7. The airspeed decreased with the extent of

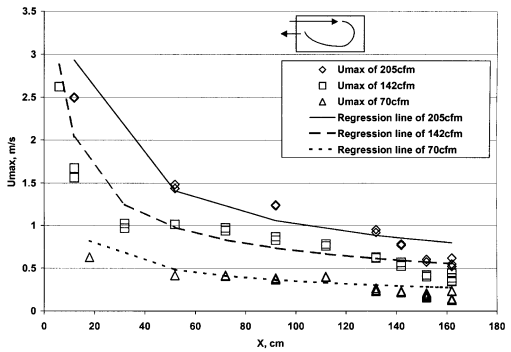

Figure 7. The maximum airspeed along enclosure ceiling.

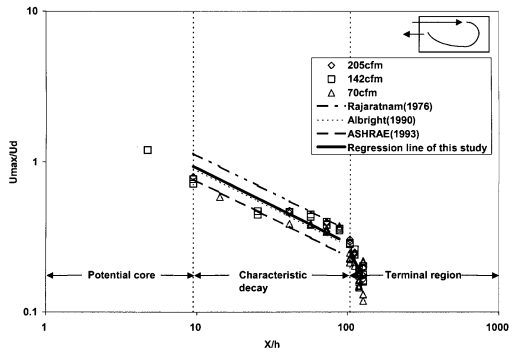

Figure 8. Normalized maximum airspeed along enclosure ceiling.

air-jet travel along the ceiling. The plots of different airspeed curve could be normalized and drawn in both log axes as a single curve (Figure 8). The region of ceiling length below 10h was potential core, where the centerline velocity was constant and approximated to U_d. The distance between 10h and 90h was characteristic decay region, and the airspeed decay equation was regressed as

$$\frac{U_{\max}}{U_d} = 2.87\sqrt{\frac{h}{x}} \quad \text{.....(14)}$$

where the throw constant C_w was between 2.35 (ASHRAE, 1993) to 3.5 (Rajaratnam, 1976).

The air-jet collapsed when it fell in terminal region with distance beyond 100h, the maximum

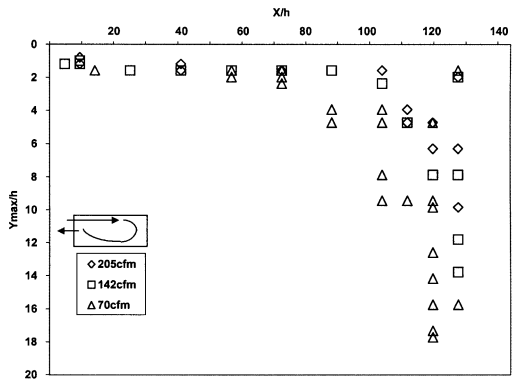

Figure 9. The maximum airspeed position along enclosure ceiling.

airspeed vanished rapidly as:

$$\frac{U_{\max}}{U_d} = 2744\frac{h^2}{x^2} \quad \text{.....(15)}$$

The variation of centerline airspeed decay appears good agreement with results obtained from Rajaratnam (1976), Albright (1990), and ASHRAE (1993).

The nondimensional maximum airspeed positions are presented in Figure 9. The positions of maximum airspeed attached to the ceiling when the air-jet remained as plane wall jet until opposite wall forced the air-jet detached from ceiling around x=100h=127cm with airflow rate of 205cfm and 142cfm. But the air-jet detached from ceiling earlier with less momentum (70cfm) while the maximum airspeed below 0.5m/s, and the position of departure was x=40h =50cm.

Profiles of jet

The profiles of airspeed in the plane wall jet are shown in Figure 10 with normalized dimensions when the airflow rate is 98cfm. These profiles located in the positions where x=0.3L, 0.5L, and 0.7L, which equals to 43h, 72h, and 101h. All locations fell into the air-jet region around characteristic decay region. The plots suggest better

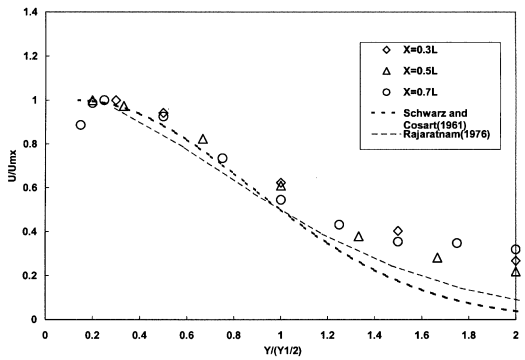

Figure 10. Normalized airspeed profiles of plane wall jet.

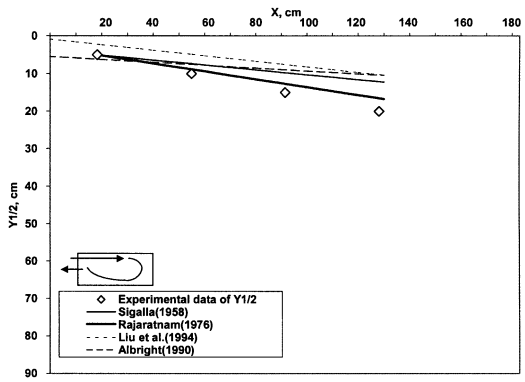

Figure 11. Half the maximum air-jet airspeed position along enclosure ceiling.

agreement with results obtained from Rajaratnam (1976) than that obtained from Schwarz and Cosart (1961).

Jet spread

The positions of half the maximum airspeed of air-jet are described in Figure 11 with airflow rate of 98cfm. The experimental results had the best agreement with Rajaratnam (1976) compared with different results of literature.

Airflow pattern

The airflow pattern within ceiling slot-ventilated enclosure has been classified into three

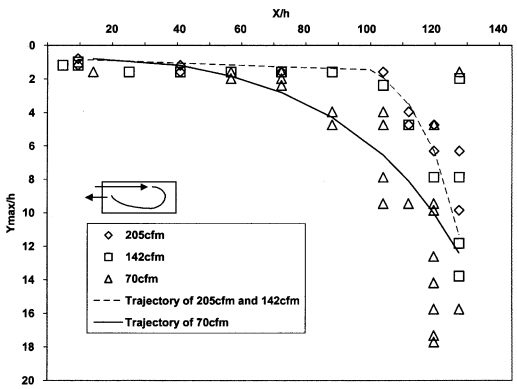

Figure 12. Airflow pattern of plane wall jet in confined enclosure.

categories as shown in Figure 2 (Jin and Ogilvie, 1990). When the airflow rate beyond the critical value of fully rotary zone, the airflow pattern is independent of airflow rate at ceiling region. The air-jet remains at ceiling region by "coanda effect" as supplied air ventilated from diffuser. The direction of air-jet curved when the opposite wall affect the airflow, and the maximum throw of air-jet will be blocked at the distance from the supply of plane wall jet at (Awbi and Setrak, 1986):

$$x_f = 0.52h(\frac{L}{h})^{1.09} = 117h = 149cm \quad .....(16)$$

For this research project, the critical values derived from the air-jet penetration throw were used. Therefore, for the chamber studied, it was assumed that transition from stagnant zone and intermediate zone to fully rotary zone occurred at $U_d=0.5/C_w*(117h/h)^{1/2}=1.88$m/s, where the airflow rate is 123cfm for the scale-model.

The airflow pattern derived from airspeed field is shown in Figure 12. The airflow pattern could be measured by the centerline velocity trajectory. The centerline trajectory of 205cfm and 142cfm remained close to ceiling until x=100h =127cm, and departure from ceiling with distance beyond that point. The results of both 205cfm and

Table 1. Comparisons of jet throw and departure distance of maximum airspeed position.

Airflow pattern	Airflow rate Q, cfm	Diffuser airspeed U_d, m/s	Reynolds number Re	Jet throw (Equation 12) L_t, cm	Distance of departure (Figure 12) L_d, cm
fully rotary zone	205	3.14	2512	413	127
fully rotary zone	142	2.18	1745	199	127
Intermediate or Stagnant zone	70	1.08	863	49	50

142cfm were in same trajectory because of both airflow rates were greater than the critical airflow rate of fully rotary zone. The discrepancy between x_f and departure distance (L_d) resulted in the x_f was derived from the air-jet separated from enclosure ceiling (Figure 3), and L_d was derived from the centerline velocity position departure from ceiling (Figure 12).

When the airflow rate below the critical airflow rate, the maximum jet throw will follow equation (12). The maximum airspeed position departure from ceiling at x=40h=50cm (Figure 12) around the end of jet throw at x=49cm (Table 1).

The consistence appears that the estimated penetration throw and the effect of opposite wall can predict the airflow pattern of isothermal plane wall jet diffused into an enclosure.

4. CONCLUSIONS

The characteristics of plane wall jet diffused into an enclosure by ventilation under isothermal condition were investigated through scale-model experiments.

The results showed the maximum airspeed decay of air-jet of equation (14) was similar to previous studies. The position of maximum airspeed was close to ceiling before the air-jet reached the end of jet throw or affected by the opposite wall. The profiles of air-jet velocity from experiments gave better agreement with results obtained from Rajaratnam (1976) than that obtained from Schwarz and Cosart (1961). The gradient of jet spread from experimental data of airspeed profiles also agreed with Rajaratnam (1976) appropriately.

Jin and Ogilvie (1990) distinguished airflow pattern of isothermal plane wall jet diffused into confined enclosure as three categories. The air-jet throw defined by terminated centerline velocity of 0.5m/s (ASHRAE, 1993) suggested the departure distance of maximum airspeed position. The airflow pattern affected by opposite wall followed by Awbi and Setrak (1986).

These agreements of air-jet characteristics can be used to predict the performance of plane wall jet diffused into a room under isothermal condition. The characteristics of air-jet in animal occupied zone affect the utility of indoor environment. And non-isothermal condition is more close to the real environment. Both subjects are important for future study.

NOMENCLATURE

C = peak velocity decay coefficient
$C_{1/2}$ = gradient of $y_{1/2}$ to x
C_d = diffuser discharge coefficient
C_w = throw constant of plane wall jet
h = diffuser width (m)
H = room height (m)
I_o = jet momentum function defined by Kaul et al. (1975) (kg/m^2-s^2)
K' = centerline velocity constant (ASHRAE,

1993)

L = room length (m)

L_d = distance from inlet when air-jet departure from maximum airspeed position (m)

L_t = air-jet throw (m)

Q = ventilation rate (m^3/s)

Re = Reynolds number, defined as $\frac{hU_d}{\nu}$

U = mean air velocity (m/s)

W = room depth (m)

x = horizontal distance from inlet wall (m)

x_0 = distance between virtual origin and inlet (m)

x_f = distance from inlet which the effect of the opposite wall is not detectable (Awbi and Setrak, 1986) (m)

y = vertical distance from floor (m)

$y_{1/2}$ = location where $U=U_{max}/2$ (m)

y_{max} = location where $U=U_{max}$ (m)

greek symbols

δ = boundary layer thickness (m)

η = $y/y_{1/2}$

subscripts

d = diffuser

max = maximum

REFERENCES

Adre, N. and L. D. Albright. 1994. Criterion for establishing similar air flow patterns (isothermal) in slotted-inlet ventilated enclosures. *Transactions of the ASAE* 37(1):235-250.

Albright, L. D. 1990. *Environmental control for animals and plants*. American Society of Agricultural Engineers, St. Joseph, MI.

ASHRAE. 1993. *ASHRAE Handbook: Fundamentals*. American Society of Heating, Refrigeration and Air-Conditioning Engineers, Atlanta, GA.

Awbi, H. B. 1991. *Ventilation of buildings*. Chapman & Hall, London.

Awbi, H. B. and A. A. Setrak. 1986. Numerical solution of ventilation air jet. Proceedings of 5thInternational Symposium on the Use of Computers for Environmental Engineering Related to Buildings, Bath, UK.

Etheridge, D. and M. Sandberg. 1996. *Building ventilation: theory and measurement*. John Wiley & Sons Ltd., West Sussex, England.

Forthmann, E. 1934. Turbulent jet expansion. National Advisory Committee for Aeronautics, Technical Memorandum No. 789. U. S. A.

Jin, Y. and J. R. Ogilvie. 1990. Near floor air speeds from center slot air inlets in swine barns. *ASAE Paper* No. 90-4004. St. Joseph, MI.

Kaul, P., W. Maltry, H. J. Muller and V. Winter. 1975. Scientific-technical principles for the control of the environment in livestock houses and stores. Translation 430. *Brit. Soc. Res. Agric. Eng.*, N.I.A.E., Silsoe, England.

Launder, B. E. and W. Rodi. 1981. The turbulent wall jet. *Progressing Aerospace Sci*. 19:81-128.

Liu, Q., S. J. Hoff., G. Maxwell, and D. S. Bundy. 1994. Numerical study of slotted wall jets with and without ceiling. *ASAE Paper* No. 94-4583. St. Joseph, MI.

Myers, G. E., J. J. Schauer, and R. H. Eustis. 1963. Plane turbulent wall jet flow development and friction factor. *J. Basic En. Transactions of ASME*. 85:47-54.

Rajaratnam, N. 1976. *Turbulent jets*. Elsevier Scientific Publishing Co., Amsterdam, Netherlands.

Sigalla, A. 1958. Measurements of skin friction in a plane turbulent wall jet. *J. the Royal Aeronautical Society* 62:873-877.

Schwarz, W. H. and W. P. Cosart. 1961. The two-dimensional turbulent wall jet. *J. Fluid Mechanics* 10(4):481-495.

Szucs, E. 1980. *Similitude and Modeling*. Elsevier Scientific Publishing Co., Amsterdam, Netherlands.

Tennekes, H. and J. L. Lumley. 1972. *A First Course in Turbulence*. MIT Press, Cambridge, MA.

Timmons, M. B., L. D. Albright, R. B. Furry and K. E. Torrance. 1980. Experimental and numerical study of air movement in slot-ventilated enclosures. *Transactions of the ASAE* 86(1): 221-239.

Tuve, G. L. 1953. Air velocities in ventilating jets. *ASHVE Transactions* 59:261.

Walker, J. N. 1977. Review of the theoretical relationships of isothermal ventilation air jets. *Transactions of the ASAE* 20:517-522.

Zhang, J. S. 1991. A fundamental study of two dimensional room ventilation flows under isothermal and non-isothermal conditions. Unpublished Ph.D. dissertation. University of Illinois at Urbana-Champaign, Urbana, IL.

收稿日期：民國 89 年 11 月 17 日
修正日期：民國 89 年 12 月 19 日
接受日期：民國 90 年 1 月 4 日